

Stabilization of Collective Motion in a Time-Invariant Flow Field

Derek A. Paley* and Cameron Peterson†

University of Maryland, College Park, MD, 20742, USA

Cooperative steering controls enable mobile sampling platforms to conduct synoptic, adaptive surveys of dynamic spatiotemporal processes by appropriately regulating the space-time separation of their sampling trajectories. Sensing platforms in the air and maritime domains can be pushed off course by strong and variable environmental dynamics. However, most existing cooperative control algorithms are based on simple motion models that do not include a flow field. Existing models that include the flow field often include speed control to compensate for the flow. In this paper, we describe a constant-speed self-propelled particle model that explicitly incorporates a time-invariant flow field. Each vehicle is represented by a Newtonian particle subject to a gyroscopic steering control. We describe the Lyapunov-based design of decentralized control algorithms that stabilize collective motion in a known flow field. In the case of a spatially variable flow, we provide an algorithm to stabilize synchronized motion, in which all of the particles move in the same direction, and circular motion, in which all of the particles orbit an inertially fixed point at a constant radius. For a spatially invariant flow, we provide an algorithm to stabilize balanced motion, in which the particle position-centroid is inertially fixed, and symmetric circular formations, in which the particle spacing around a circle is temporally regulated. Via the latter algorithm we provide a method of stabilizing a circular formation in which the particles are evenly spaced in time and the formation is centered on a moving target. The theoretical results are illustrated with two numerical examples based on applications in environmental monitoring and target surveillance.

*Assistant Professor, Department of Aerospace Engineering; dpaley@umd.edu. Senior Member AIAA.

†Graduate student, Department of Aerospace Engineering; cammykai@yahoo.com.

Nomenclature

N	Number of particles
r_k	Position of particle k
\dot{r}_k	Inertial velocity of particle k
s_k	Speed of particle k
f_k	Flow velocity at position r_k
θ_k	Orientation of the velocity of particle k relative to the flow
γ_k	Orientation of the inertial velocity of particle k
ψ_k	Time-phase of of particle k in a circular orbit
T	Period of revolution around a circular orbit
c_k	Center of circle traversed by particle k
ω_0	Constant angular rate
P	$N \times N$ projector matrix
P_k	k th row of matrix P
K	Control gain
i	Imaginary unit

Subscript

j, k Particle and phase indices, $1, \dots, N$

I. Introduction

Autonomous vehicles provide a robust sensing platform for synoptic and adaptive sampling of spatiotemporal processes in the air and sea. Decentralized control algorithms that coordinate the sampling trajectories of multiple vehicles enhance the sensory performance of the entire fleet by appropriately regulating the space-time separation of sample points.¹ A major impediment to the regulation of trajectory separation is the presence of an external flow field—e.g., ocean currents or atmospheric winds. Cooperative control algorithms that are effective in weak flow fields often fail in moderate to strong flows. In this paper, we provide decentralized algorithms that stabilize collective motion in a time-invariant flow field. We assume that (1) the flow field is known and (2) the flow field is weaker than the particle speed relative to the flow, although these theoretical restrictions have been successfully lifted in numerical simulations. The extension of these results to strong and variable flows is the subject of ongoing analysis.

Robust coordination of multiple vehicles in the absence of flow can be produced by co-

operative control of a dynamic motion model in which each vehicle is represented by a Newtonian particle moving at constant speed in a plane.²⁻⁴ Each particle is subject to a gyroscopic (steering) control that determines the rate of rotation of the particle velocity. Using a particle framework, theoretically justified algorithms^{5,6} generate symmetric formations in which the relative positions and relative orientations of all vehicles are optimized for sampling performance—under very mild assumptions on the inter-vehicle communication. These algorithms have been successfully demonstrated in multiple at-sea experiments with autonomous underwater vehicles.^{7,8}

Analysis of ocean-sampling field experiments highlights the need to develop theoretically justified algorithms that stabilize collective motion in the presence of a strong and variable flow field.⁹ Underwater vehicles routinely encounter ocean currents that match or exceed vehicle speed. These currents push vehicles away from their desired trajectories and compress/expand the space-time separation of vehicle trajectories, leading to a degradation of overall sampling performance. Strong currents that vary substantially in time are especially challenging because of the inherent uncertainty in current forecasts. The derivation of cooperative control and estimation algorithms for strong and variable currents is outside the scope of this paper. We focus instead on what to do in the presence of a known, time-invariant flow in which an underwater or aerial vehicle has strictly positive speed-over-ground.

We utilize a planar model that explicitly incorporates a time-invariant flow field.^{10,11} Each vehicle is represented by a Newtonian particle subject to a gyroscopic steering control. We present a Lyapunov-based design of decentralized control algorithms that stabilize collective motion in a known flow field. The control design is a direct extension of the framework introduced for the flow-free model with all-to-all communication.⁵ Accordingly, all of the results presented herein extend naturally to limited communication topologies that may be time-varying and/or directed.⁶ Likewise, our focus on circular motion is for brevity only; the framework has been extended to motion on convex loops in a flow field.¹²

In the case of a spatially variable flow, we provide an algorithm to stabilize synchronized motion, in which all of the particles move in the same direction, and circular motion, in which all of the particles orbit an inertially fixed point at a constant radius. In addition, we show how to prescribe the center of a circular formation using a virtual particle. For a spatially invariant flow, we provide an algorithm to stabilize balanced motion, in which the particle position-centroid is inertially fixed, and symmetric circular formations, in which the particle spacing around a circle is temporally regulated. Via the latter algorithm we provide a method of stabilizing a circular formation in which the particles are evenly spaced in time. These motion primitives collectively form a foundation upon which more complex mission-specific trajectories can be constructed.

The results presented here contribute to a body of research results that highlight the

impact of a flow field on motion-planning for unmanned vehicles.^{13–17} For example, it has been shown that, unlike the no wind case, the minimum time paths from a known start point to a known endpoint consist of three arcs.¹⁴ Furthermore, onboard-camera tilt and pan are minimized by an elliptical platform trajectory that spirals in towards a target.¹⁶ We provide control laws to stabilize a circular formation centered on an inertially-fixed point—results that are applicable to stabilizing a formation of constant-speed vehicles to a circular orbit centered on a target moving at a constant velocity.^{18–20} An alternate algorithm exists to match the average vehicle velocity to a time-invariant reference and, with the use of an outer-loop control, to a known time-varying reference.¹⁸

The problem of tracking a moving target with a circular formation of variable-speed vehicles has also been studied recently.^{21,22} The trajectory of a vehicle can be controlled through Lyapunov guidance vector fields chosen to satisfy a specific candidate Lyapunov function and thereby provide globally stable paths.²¹ Guidance vector fields containing a limit cycle allow multiple vehicles to orbit a constant-velocity target at a desired stand-off radius. For vehicles without speed control traveling in a circular formation in wind, only regulation of temporal and not spatial separation is possible. The notion of temporal regulation of constant-speed vehicles in a circular formation has been studied in the context of a sliding-mode design of a solution to the target-tracking problem in which multiple vehicles orbit a target at regular intervals.²⁰ We further explore this notion, utilizing in our control design concepts from the literature on cooperative control via coupled phase oscillator models.^{5,6}

The paper has the following outline. In Section II we describe a self-propelled particle model that explicitly incorporates a time-invariant flow field. In Section III we provide decentralized control algorithms to stabilize, respectively, a synchronized formation in a spatially variable field and a balanced formation in a spatially invariant field. In Section IV, we provide an algorithm to stabilize a circular formation in a spatially variable field. In Section V we provide algorithms to isolated circular formations in which the temporal separation of particles in the formation is temporally regulated in a spatially invariant field. In Section VI we provide results from numerical simulations related to applications in environmental monitoring and target surveillance. In Section VII, we summarize the results and provide indications of ongoing and future work, which includes the stabilization of collective motion in a time-varying flow field.

II. A model of particles in a flow field

In this paper we study a dynamic model of N self-propelled particles in a time-invariant flow field. Each particle is subject to a steering control produced by a gyroscopic force

or, equivalently,

$$\sin \theta_k = s_k \sin \gamma_k - \langle f_k, i \rangle \quad (4)$$

$$\cos \theta_k = s_k \cos \gamma_k - \langle f_k, 1 \rangle, \quad (5)$$

which imply

$$\tan \gamma_k = \frac{\sin \theta_k + \langle f_k, i \rangle}{\cos \theta_k + \langle f_k, 1 \rangle}. \quad (6)$$

Differentiating (6) with respect to time along solutions of (1) and solving for $\dot{\gamma}_k$ using (4) and (5) we obtain

$$\begin{aligned} \dot{\gamma}_k &= (\cos \theta_k \cos \gamma_k + \sin \theta_k \sin \gamma_k) s_k^{-1} \dot{\theta}_k + \langle \dot{f}_k, i \rangle s_k^{-1} \cos \gamma_k - \langle \dot{f}_k, 1 \rangle s_k^{-1} \sin \gamma_k \\ &= (1 - s_k^{-1} \langle e^{i\gamma_k}, f_k \rangle) u_k + \langle f'_k, i \rangle \triangleq \nu_k, \end{aligned} \quad (7)$$

where we used $\dot{f}_k = f'_k \dot{r}_k$.

We view ν_k defined in (7) as a control input, since one can compute u_k according to

$$u_k = \frac{\nu_k - \langle f'_k, i \rangle}{1 - s_k^{-1} \langle e^{i\gamma_k}, f_k \rangle}. \quad (8)$$

Note that (8) is well defined since the denominator is never equal to zero. We prove this fact by contradiction. Suppose the denominator is equal to zero, then

$$s_k = \langle e^{i\gamma_k}, f_k \rangle = \langle e^{i\theta_k} + f_k, f_k \rangle s_k^{-1}, \quad (9)$$

which implies

$$s_k^2 = \langle e^{i\theta_k} + f_k, e^{i\theta_k} + f_k \rangle = \langle e^{i\theta_k} + f_k, f_k \rangle \quad (10)$$

and, after canceling terms,

$$1 + \langle e^{i\theta_k}, f_k \rangle = 0. \quad (11)$$

However, (11) is a contradiction since $|\langle e^{i\theta_k}, f_k \rangle| \leq |f_k| < 1$, by assumption.

As a consequence of this analysis, it is equivalent to write (1) as

$$\begin{aligned} \dot{r}_k &= s_k e^{i\gamma_k} \\ \dot{\gamma}_k &= \nu_k, \end{aligned} \quad (12)$$

where ν_k is defined in (7). The model (12) is a self-propelled particle model with a variable speed $s_k = |e^{i\theta_k} + f_k| > 0$ and steering control ν_k . Note, the speed s_k depends on the particle phase γ_k and, possibly, the position r_k ; the speed s_k is not a control variable.

In the following two examples, we calculate s_k and u_k for a uniform flow and a non-uniform flow, respectively.

Example 1. Uniform flow Without loss of generality, we align the positive real axis of the inertial frame with the orientation of a uniform flow, so that $f_k = \beta \in \mathbb{R}$, $|\beta| < 1$. We calculate

$$\begin{aligned} s_k &= \sqrt{\operatorname{Re}\{(\beta + e^{i\theta_k})(\beta + e^{-i\theta_k})\}} \\ &= \sqrt{1 + \beta^2 + 2\beta \cos \theta_k}. \end{aligned} \quad (13)$$

We express s_k as a function of γ_k and $f_k = \beta$ by substituting (5) into (13) and rearranging the result to obtain the quadratic equation

$$s_k^2 - 2\beta \cos \gamma_k s_k + \beta^2 - 1 = 0,$$

which has the solution (using the positive root since $s_k > 0$)

$$s_k = \beta \cos \gamma_k + \sqrt{1 - \beta^2 \sin^2 \gamma_k}. \quad (14)$$

Note, s_k for a uniform flow field is a function of γ_k only, and not r_k . In order to find u_k as a function of ν_k , substitute $f_k = \beta$ (and $f'_k = 0$) into (8) to obtain

$$u_k = \frac{\nu_k}{1 - \beta s_k^{-1} \cos \gamma_k}. \quad (15)$$

Example 2. Non-uniform flow Let $f_k = \beta_k + i\alpha_k$, where $\beta_k = \langle f_k, 1 \rangle$ and $\alpha_k = \langle f_k, i \rangle$ are the real and imaginary parts, respectively, of a spatially variable flow field. We have

$$\begin{aligned} s_k &= \sqrt{\operatorname{Re}\{(e^{i\theta_k} + \beta_k + i\alpha_k)(e^{-i\theta_k} + \beta_k - i\alpha_k)\}} \\ &= \sqrt{1 - \beta_k^2 - \alpha_k^2 + 2s_k(\alpha_k \sin \gamma_k + \beta_k \cos \gamma_k)}, \end{aligned} \quad (16)$$

where we used (4) and (5). Squaring both sides of (16) and solving the resulting quadratic equation (using the positive root since $s_k > 0$) yields

$$\begin{aligned} s_k &= \alpha_k \sin \gamma_k + \beta_k \cos \gamma_k + \sqrt{1 - (\alpha_k \cos \gamma_k - \beta_k \sin \gamma_k)^2} \\ &= \langle e^{i\gamma_k}, f_k \rangle + \sqrt{1 - \langle ie^{i\gamma_k}, f_k \rangle^2}. \end{aligned} \quad (17)$$

Note s_k depends here on both γ_k and r_k .

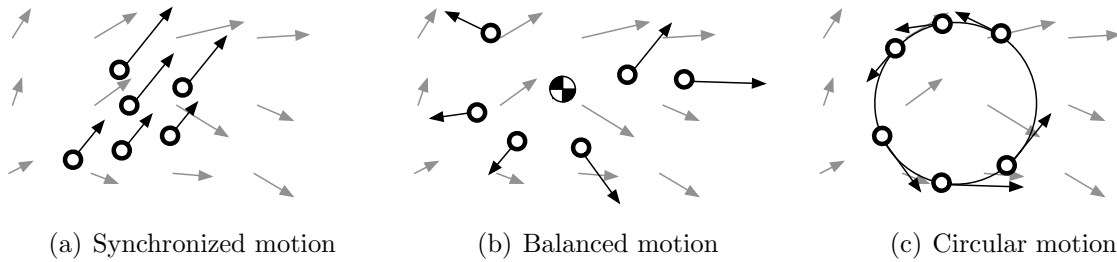


Figure 2. Three motion primitives of the particle model in a time-invariant flow. The arrow attached to each particle represents its inertial velocity. (a) In synchronized motion, the particles move in the same direction with arbitrary separation. (b) In balanced motion, the centroid of the particle positions is fixed. (c) In circular motion, the particles travel in the same direction around a circle with fixed center.

In order to compute u_k for a non-uniform flow field, let $r_k = x_k + iy_k$, which implies

$$f'_k = \frac{\partial \beta_k}{\partial x_k} + i \frac{\partial \alpha_k}{\partial y_k}. \quad (18)$$

Substituting (18) into (8) completes the calculation. In the simulations in Sections III and IV, we use a smooth, periodic flow field

$$f_k = a_0 \sin(2\pi\omega x_k - \varphi_0) + i \cos(2\pi\omega y_k - \varphi_0), \quad (19)$$

which is parametrized by a_0 , ω , and φ_0 .

III. Phase synchronization and balancing

Three motion primitives of the particle model (12) illustrated in Figure 2 are synchronized, balanced, and circular motions.⁵ In this section, we study synchronized and balanced motions and, in the next section, we study circular motions. In synchronized motion, all of the phases γ_k , $k = 1, \dots, N$, are equal and the particles move in the same direction with arbitrary separation. In balanced motion, the centroid of the particle positions, $p_r \triangleq (1/N) \sum_{j=1}^N r_j$, is fixed, which implies that the quantity $p_{\dot{r}} \triangleq (1/N) \sum_{j=1}^N \dot{r}_j = \dot{p}_r$ is zero. A Lyapunov-based control framework exists to stabilize synchronized and balanced motions in a flow-free particle model.⁵ In this section, we extend the flow-free framework to stabilize synchronized and balanced motions in a time-invariant flow field.

Synchronized motion corresponds to the maximum of the potential^c

$$U(\boldsymbol{\gamma}) \triangleq \frac{1}{2} |p_{\boldsymbol{\gamma}}|^2, \quad (20)$$

^cWe drop the subscript and use bold to represent an $N \times 1$ matrix, e.g., $\boldsymbol{\gamma} = (\gamma_1, \dots, \gamma_N)^T$.

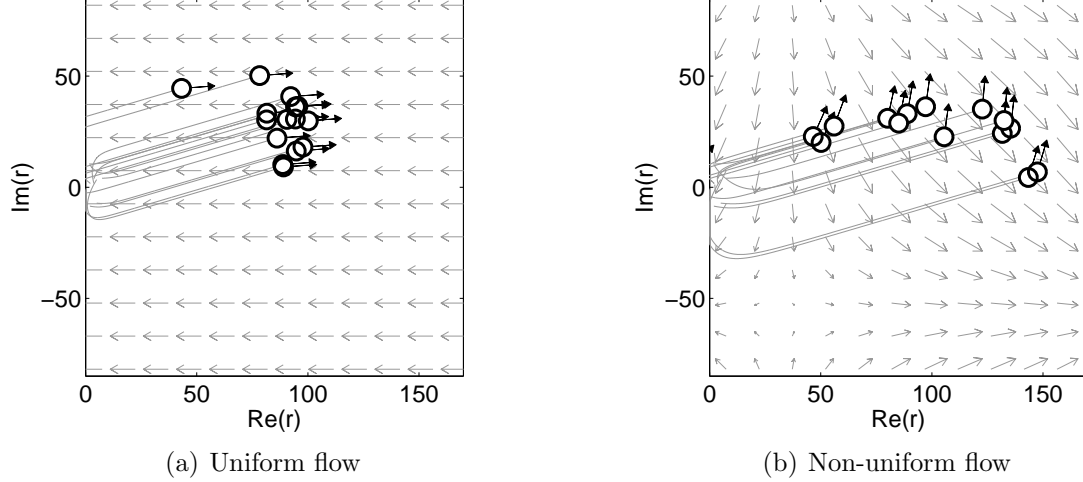


Figure 3. Synchronization of the particle phase γ using the control (22) with $N = 15$ and $K = -0.1$ yields a parallel formation with arbitrary separation. The arrow attached to each particle represents its velocity relative to the flow. (a) Uniform flow field $f_k = -0.75$ (assuming unit particle speed). (b) Non-uniform flow field (19) with $a_0 = -0.75$, $\omega = 1/360$, and $\varphi_0 = 10$.

where

$$p_\gamma \triangleq \frac{1}{N} \sum_{j=1}^N e^{i\gamma_j} \quad (21)$$

is the centroid of the phasors $e^{i\gamma_k}$, $k = 1, \dots, N$. The following result is proven using Lyapunov stability theory.

Theorem 1. *The closed loop particle model (12) with the gradient control*

$$\nu_k = -K \frac{\partial U}{\partial \gamma} = -K \langle p_\gamma, i e^{i\gamma_k} \rangle, \quad K < 0, \quad (22)$$

forces convergence of all solutions to the critical set of U . The set of synchronized motions are asymptotically stable and every other equilibrium is unstable.

Proof. See [5, Theorem 1]. □

We illustrate Theorem 1 in Figure 3.

Theorem 1 provides a decentralized synchronization algorithm for a non-uniform flow field. In order to stabilize balanced motions, we assume that the flow is uniform (see Example 1). We stabilize balanced solutions of (12) with $f_k = \beta \in \mathbb{R}$ by minimizing the potential¹⁰

$$V(\mathbf{r}, \boldsymbol{\gamma}) = \frac{1}{2} |p_{\dot{\mathbf{r}}}|^2, \quad (23)$$

where

$$p_{\dot{\mathbf{r}}} \triangleq \frac{1}{N} \sum_{j=1}^N s_j e^{i\gamma_j} \quad (24)$$

is the centroid of the particle velocities. Note $V(\mathbf{r}, \boldsymbol{\gamma}) = 0$ when $p_r = 0$, i.e., the centroid of particle positions is fixed, and positive otherwise. The time-derivative of $V(\mathbf{r}, \boldsymbol{\gamma})$ along solutions of (12) is

$$\dot{V} = \langle p_{\dot{r}}, \dot{p}_{\dot{r}} \rangle = \sum_{j=1}^N \langle p_{\dot{r}}, \dot{s}_j e^{i\gamma_j} + s_j i e^{i\gamma_j} \dot{\gamma}_j \rangle, \quad (25)$$

where, for a uniform flow,

$$\dot{s}_k = \delta_k s_k \dot{\gamma}_k, \quad \delta_k \triangleq \frac{-\beta \sin \gamma_k}{\sqrt{1 - \beta^2 \sin^2 \gamma_k}}. \quad (26)$$

Substituting (26) into (25) yields

$$\dot{V} = \sum_{j=1}^N \langle p_{\dot{r}}, (\delta_j + i) e^{i\gamma_j} \rangle s_j \nu_j. \quad (27)$$

Lyapunov analysis leads to the following result.

Theorem 2. *The particle model (12) with $f_k = \beta$, $|\beta| < 1$, and the control*

$$\nu_k = -K \langle p_{\dot{r}}, (\delta_k + i) e^{i\gamma_k} \rangle s_k, \quad K > 0, \quad (28)$$

where δ_k is defined in (26), asymptotically stabilizes the set of balanced motions, which is the set of motions for which the centroid of particle positions is fixed.

Proof. Substituting (28) into (27) yields

$$\dot{V} = -K \sum_{j=1}^N \langle p_{\dot{r}}, (\delta_j + i) e^{i\gamma_j} \rangle^2 s_j^2 \leq 0. \quad (29)$$

By the invariance principle, all of the solutions of (12) with the control (28) converge to the largest invariant set in which

$$\langle p_{\dot{r}}, (\delta_k + i) e^{i\gamma_k} \rangle \equiv 0. \quad (30)$$

In this set, $\dot{\gamma}_k = 0$ and $\dot{s}_k = 0$, which implies $p_{\dot{r}}$ is constant. Since $\delta_k + i \neq 0$ (δ_k is real), then the invariance condition (30) is satisfied for all $k = 1, \dots, N$, only when $p_{\dot{r}} = 0$. \square

IV. Stabilization of circular formations

In this section we describe a decentralized algorithm to stabilize a circular formation in which all particles orbit an inertially fixed point at a fixed radius. The center of the circular formation can be prescribed by introducing a virtual particle, as described below. These

results represent a direct extension of the flow-free framework⁵ to the particle model (12).

In the absence of flow, i.e., using the model (1), setting u_k equal to a constant, $\omega_0 \neq 0$, drives particle k around a circle of radius ω_0^{-1} and fixed center⁵

$$c_k \triangleq r_k + \omega_0^{-1} i \frac{\dot{r}_k}{|\dot{r}_k|}. \quad (31)$$

In the presence of a time-invariant flow field, we have the following result.¹⁰

Lemma 1. *The model (12) with the control*

$$\nu_k = \omega_0 s_k \quad (32)$$

drives particle k around a circle of radius ω_0^{-1} centered at $c_k(t) = r_k(0) + \omega_0^{-1} i e^{i\gamma_k(0)}$.

Proof. We derive the control ν_k that steers the particle around a circle by differentiating (31) along solutions of (12). This results in

$$\dot{c}_k = s_k e^{i\gamma_k} - \omega_0^{-1} e^{i\gamma_k} \nu_k = (s_k - \omega_0^{-1} \nu_k) e^{i\gamma_k}. \quad (33)$$

Substituting (32) into (33) yields $\dot{c}_k = 0$, which proves that the center of the circle is fixed. To complete the proof, we observe that the radius of the circle is $|c_k(t) - r_k(0)| = \omega_0^{-1}$. \square

A circular formation is a solution of the particle model (12) in which all of the particles orbit the same circle in the same direction. Let $\mathbf{1} \triangleq (1, \dots, 1)^T \in \mathbb{R}^N$. In a circular formation, $c_k = c_j$ for all pairs j and k , which implies that a circular formation satisfies the condition $P\mathbf{c} = 0$,⁵ where P is an $N \times N$ projection matrix given by

$$P = \text{diag}\{\mathbf{1}\} - \frac{1}{N} \mathbf{1}\mathbf{1}^T. \quad (34)$$

Note, P projects an element of \mathbb{C}^N into the subspace complementary to the span of $\mathbf{1}$.

We derive a decentralized control that stabilizes a circular formation by considering the potential⁵

$$S(\mathbf{r}, \boldsymbol{\gamma}) \triangleq \frac{1}{2} \langle \mathbf{c}, P\mathbf{c} \rangle. \quad (35)$$

Note $S \geq 0$, with equality only when $\mathbf{c} = c_0 \mathbf{1}$, $c_0 \in \mathbb{C}$. The time derivative of S along solutions of (12) is

$$\dot{S} = \sum_{j=1}^N \langle \dot{c}_j, P_j \mathbf{c} \rangle = \sum_{j=1}^N \langle e^{i\gamma_j}, P_j \mathbf{c} \rangle (s_j - \omega_0^{-1} \nu_j), \quad (36)$$

where P_k denotes the k th row of the matrix P . The following result provides a control

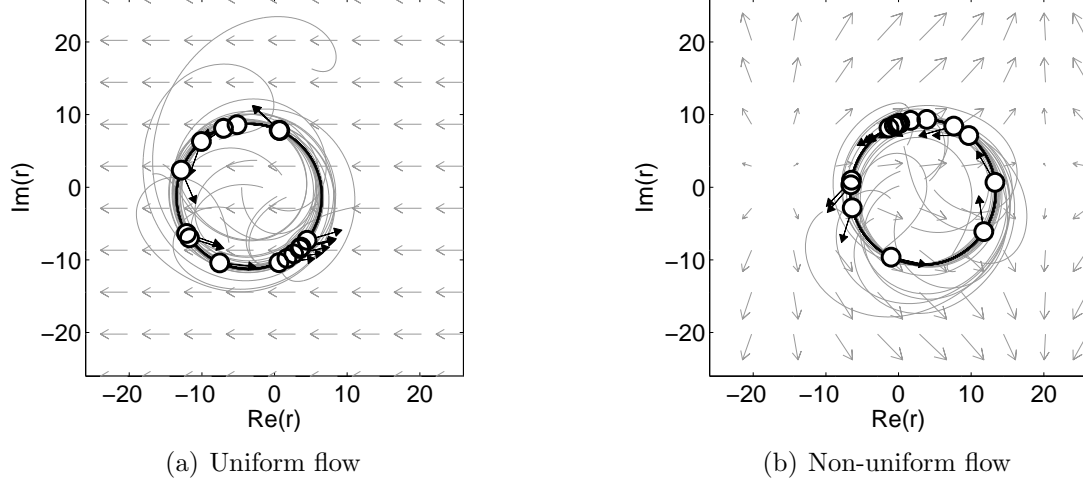


Figure 4. Stabilization of a circular formation using the control (37) with $N = 15$ and $K = 0.1$. The arrow attached to each particle represents its velocity relative to the flow. (a) Uniform flow with $\beta = -0.75$ (assuming unit particle speed). (b) Non-uniform flow field (19) with $a_0 = -0.75$, $\omega = 5/360$, and $\varphi_0 = 8$.

algorithm to stabilize a circular formation in a time-invariant flow.¹⁰ It extends [5, Theorem 2], which provides a circular-formation algorithm for the flow-free particle model.

Theorem 3. *All solutions of the particle model (12) with the control*

$$\nu_k = \omega_0(s_k + K\langle P_k \mathbf{c}, e^{i\gamma_k} \rangle), \quad K > 0, \quad (37)$$

converge to a circular formation with radius ω_0^{-1} and direction determined by the sign of ω_0 .

Proof. The potential $S(\mathbf{r}, \boldsymbol{\gamma})$ is positive definite and proper in the space of relative circle centers. Substituting (37) into (36) yields

$$\dot{S} = -K \sum_{j=1}^N \langle P_k \mathbf{c}, e^{i\gamma_k} \rangle^2 \leq 0.$$

By the invariance principle, all of the solutions of (12) with control (37) converge to the largest invariant set, Λ , in which

$$\langle P_k \mathbf{c}, e^{i\gamma_k} \rangle \equiv 0. \quad (38)$$

In this set, $\dot{\gamma}_k = \omega_0 s_k$ and $\dot{c}_k = 0$. Therefore, in order to satisfy the invariance condition, (38), all of the solutions in Λ must satisfy $P\mathbf{c} = 0$, which is the circular-formation condition. Application of Lemma 1 completes the proof. \square

We illustrate Theorem 3 in Figure 4.

The control algorithm described in Theorem 3 depends not on absolute positions but on *relative* positions, i.e., $r_k - r_j$, for any pair k and j . Consequently, the algorithm preserves

the symmetry of the closed-loop particle model (12) that renders the model invariant to rigid translation of all of the particles.² This property of the control algorithm implies the steady-state center of the circle depends only on initial conditions. For applications in path-planning for autonomous vehicles, there exists the need to specify the steady-state center of the vehicle formation in the presence of flow. This need also arises in the context of tracking a target moving at a constant velocity. We describe next a symmetry-breaking algorithm that provides this capability.¹⁰

Following the flow-free development,⁶ we introduce a virtual particle labelled with $k = 0$ that serves as a reference. The virtual particle dynamics,

$$\begin{aligned}\dot{r}_0 &= s_0 e^{i\gamma_0} \\ \dot{\gamma}_0 &= \omega_0 s_0,\end{aligned}\tag{39}$$

where $\omega_0 \neq 0$, are independent of the dynamics of the particles. In the solution to (39), particle 0 orbits a circle of radius $|\omega_0|^{-1}$ with fixed center $c_0 = r_0(0) + \omega_0^{-1} i e^{i\gamma_0(0)}$. Assume the virtual particle's relative state variables are available to a nonempty subset of the particles, which we call the informed particles. Let $a_{k0} = 1$ if particle k is an informed particle and $a_{k0} = 0$ otherwise.

Consider augmenting the potential S defined in (35) with the quadratic potential⁶

$$S_0(\mathbf{r}, \boldsymbol{\gamma}) = \frac{1}{2} \sum_{j=1}^N a_{j0} |c_j - c_0|^2,$$

which is minimized when $c_j = c_0$ for all $\{j \mid j \in 1, \dots, N, a_{j0} = 1\}$. The time-derivative of $\tilde{S}(\mathbf{r}, \boldsymbol{\gamma}) \triangleq S(\mathbf{r}, \boldsymbol{\gamma}) + S_0(\mathbf{r}, \boldsymbol{\gamma})$ along solutions of (12) is

$$\dot{\tilde{S}} = \sum_{j=1}^N (\langle e^{i\gamma_j}, P_j \mathbf{c} \rangle + a_{j0} \langle e^{i\gamma_j}, c_j - c_0 \rangle) (s_j - \omega_0^{-1} \nu_j)\tag{40}$$

This analysis leads to the following corollary to Theorem 3.¹⁰

Corollary 1. *Let $c_0 = r_0(0) + \omega_0^{-1} i e^{i\gamma_0(0)}$ be the fixed reference provided by a virtual particle, $k = 0$, whose dynamics are given by (39). Let $a_{k0} = 1$ equal one if particle k is informed of the reference and $a_{k0} = 0$ otherwise. If there is at least one informed particle, then all solutions of the particle model (12) with the control*

$$\nu_k = \omega_0 (s_k + K (\langle e^{i\gamma_k}, P_k \mathbf{c} \rangle + a_{k0} \langle e^{i\gamma_k}, c_k - c_0 \rangle)), \quad K > 0,\tag{41}$$

converge to a circular formation centered at c_0 with radius ω_0^{-1} and direction determined by

the sign of ω_0 .

Proof. With the control (41), the time-derivative of the augmented potential $\tilde{S}(\mathbf{r}, \boldsymbol{\gamma})$ satisfies

$$\dot{\tilde{S}} = -K \sum_{j=1}^N (\langle e^{i\gamma_k}, P_k \mathbf{c} \rangle + a_{k0} \langle e^{i\gamma_k}, c_k - c_0 \rangle)^2 \leq 0.$$

By the invariance principle, all solutions converge to the largest invariant set for which

$$\langle e^{i\gamma_k}, P_k \mathbf{c} \rangle + a_{k0} \langle e^{i\gamma_k}, c_k - c_0 \rangle \equiv 0 \quad (42)$$

for $k = 1, \dots, N$. In this set, $\dot{\gamma}_k = \omega_0 s_k$ and $\dot{c}_k = 0$.

If $a_{k0} = 0$ for at least one but not all $k \in \{1, \dots, N\}$, then the invariance condition (42) is satisfied only if $P_k \mathbf{c} = 0$. This implies \mathbf{c} is in the span of $\mathbf{1}$, i.e. $c_k = c_j$ for all pairs k and j . For all k with $a_{k0} = 1$, the invariance condition becomes

$$\langle e^{i\gamma_k}, c_k - c_0 \rangle \equiv 0,$$

which holds only if $c_k = c_0$. This implies $c_k = c_0 \mathbf{1}$.

If $a_{k0} = 1$ for all k , then the invariance condition becomes

$$\langle e^{i\gamma_k}, \tilde{P}_k \mathbf{c} \rangle \equiv 0, \quad (43)$$

where \tilde{P} is the $(N+1) \times (N+1)$ projection matrix defined as in (34). The condition (43) is satisfied only if $c_k = c_0$ for all k , which completes the proof. \square

Corollary 1 also provides a procedure to stabilize a circular formation centered on a target moving at a constant velocity. Let \mathcal{B} represent a reference frame that is not rotating with respect to the inertial frame \mathcal{I} and whose origin O' is moving relative to O at a constant velocity b_0 equal to the target velocity. Note \mathcal{B} is an inertial frame and the target position is a fixed point in \mathcal{B} . Let r'_k denote the position of particle k relative to O' . We have

$$\dot{r}'_k = e^{i\theta_k} + f_k - b_0. \quad (44)$$

The equations of motion expressed in frame \mathcal{B} are

$$\begin{aligned} \dot{r}'_k &= e^{i\theta_k} + f'_k \\ \dot{\theta}_k &= u_k, \end{aligned} \quad (45)$$

where $f'_k \triangleq f_k - b_0$. Therefore, the particle dynamics in frame \mathcal{B} are equivalent to (12) with

r_k replaced by r'_k and f_k replaced by f'_k . Applying the control (41) with c_0 equal to the target position in frame \mathcal{B} stabilizes a circular formation centered on the target. We illustrate this result in Section VI.

V. Symmetric circular formations

In this section we provide an algorithm that steers a particle collective to a circular formation and, simultaneously, regulates the separation of the particles around the circle. To do this we introduce a phase variable that represents the progress of a particle around the circle.²³ The development of Lyapunov-based algorithms utilizing the phase variable to stabilize symmetric formations is a direct extension of the flow-free framework.⁵ In previous work, control laws are provided to regulate the along-track separation of the particles in the absence of flow; here, we provide a control algorithm to regulate the temporal separation of particles in a uniform flow field.

Recall from Example 1 that the speed of a particle in uniform flow is independent of the particle position, i.e., $s_k = s(\gamma_k)$ for all $k = 1, \dots, N$. According to Lemma 1, the closed-loop phase dynamics

$$\dot{\gamma}_k = \omega_0 s_k \quad (46)$$

drive particle k around a circular trajectory. Integrating (46) by separation of variables, we obtain

$$t = \frac{1}{\omega_0} \int_0^{\gamma_k(t)} \frac{d\gamma}{s(\gamma)}, \quad (47)$$

which is an implicit expression for the solution to (46), $\gamma_k(t)$.

The key observation is that we can use a quantity proportional to the right-hand side of (47) as measure of the *temporal* separation of solutions to (46). We call this quantity the *time-phase*, ψ_k , defined by¹¹

$$\psi_k = \frac{2\pi}{\omega_0 T} \int_0^{\gamma_k} \frac{d\gamma}{s(\gamma)}, \quad (48)$$

where $T > 0$ is the period of a single revolution,

$$T = \frac{1}{\omega_0} \int_0^{2\pi} \frac{d\gamma}{s(\gamma)}. \quad (49)$$

(A similar quantity, called the curve-phase, has been previously used to measure arc-length separation along a closed curve.^{4,23}) The function $\gamma_k = \gamma_k(\psi_k)$ implicitly defined in (48) is a diffeomorphism, as long as $s(\gamma) > 0$.

We now incorporate the time-phase variable into the design of a formation control. The

time-derivative of (48) along solutions of (12) is

$$\dot{\psi}_k = \frac{2\pi}{T}(\omega_0 s_k)^{-1} \nu_k. \quad (50)$$

Let $U(\boldsymbol{\psi})$ represent a smooth potential that satisfies $U(\boldsymbol{\psi} + \psi_0 \mathbf{1}) = U(\boldsymbol{\psi})$, which is the condition for rotational symmetry. Rotational symmetry implies $\sum_{j=1}^N \frac{\partial U}{\partial \psi_j} = 0$.⁵ Consider the composite potential

$$V(\mathbf{r}, \boldsymbol{\gamma}) = S(\mathbf{r}, \boldsymbol{\gamma}) + \frac{T}{2\pi} U(\boldsymbol{\psi}),$$

where $S(\mathbf{r}, \boldsymbol{\gamma})$ is the circular-formation Lyapunov potential defined in (35). Using (50) and the rotational symmetry of $U(\boldsymbol{\psi})$ we find

$$\begin{aligned} \dot{V} &= \sum_{j=1}^N \langle e^{i\gamma_j}, P_j \mathbf{c} \rangle (s_j - \omega_0^{-1} \nu_j) + \frac{T}{2\pi} \frac{\partial U}{\partial \psi_j} \dot{\psi}_j \\ &= \sum_{j=1}^N \left(s_j \langle e^{i\gamma_j}, P_j \mathbf{c} \rangle - \frac{\partial U}{\partial \psi_j} \right) (1 - (\omega_0 s_j)^{-1} \nu_j). \end{aligned} \quad (51)$$

Choosing the control law

$$\nu_k = \omega_0 s_k \left(1 + K \left(s_j \langle e^{i\gamma_k}, P_k \mathbf{c} \rangle - \frac{\partial U}{\partial \psi_k} \right) \right), \quad K > 0, \quad (52)$$

yields

$$\dot{S} = -K \sum_{j=1}^N (s_j - \omega_0^{-1} \nu_j)^2 \leq 0$$

and

$$\dot{S} = 0 \Leftrightarrow \nu_k = \omega_0 s_k.$$

The following result is obtained using the invariance principle.⁵

Theorem 4. *Consider the particle model (12) with uniform flow $f_k = \beta$ and a smooth, rotationally symmetric phase potential $U(\boldsymbol{\psi})$. The control law (52) enforces convergence of all solutions to the set of circular formations where all particles move around a circle of radius ω_0^{-1} and direction given by the sign of ω_0 with a phase arrangement in the critical set of $U(\boldsymbol{\psi})$. Every isolated minimum of $U(\boldsymbol{\psi})$ defines an asymptotically stable set of circular formations. Every circular formation where $U(\boldsymbol{\psi})$ does not reach a minimum is unstable.*

Proof. See [5, Theorem 3]. □

As an example, we describe a phase potential $U(\boldsymbol{\psi})$ that isolates symmetric patterns of the time-phase variables, $\boldsymbol{\psi}$. An (M, N) -pattern, where M is a divisor of N , is a symmetric

arrangement of N phases consisting of M clusters uniformly spaced around the unit circle, each with N/M synchronized phases.⁵ For any N , there exist at least two symmetric patterns: the $(1, N)$ -pattern, which is the synchronized state, and the (N, N) -pattern—the splay state—characterized by N phases uniformly spaced around the unit circle. In a splay pattern of time-phase variables, the particles are uniformly separated in time as they orbit a circular formation in a flow field. For example, a time-splay configuration in which the particles are labeled sequentially around the formation satisfies²⁰

$$\begin{aligned}\gamma_k(t) &= \gamma_{k+1}(t - T/N), \quad k = 1, \dots, N - 1, \\ \gamma_N(t) &= \gamma_1(t - T/N),\end{aligned}\tag{53}$$

where T is the period of revolution defined in 49). This type of formation has been explored previously in the context of the particle model (12),^{11,20} although we are not aware of any other algorithm proven to force convergence to a time-splay formation. Note, in our framework, we do not impose the requirement of sequential labeling nor do we require control of particle speed.

Theorem 5. [5, Theorem 6] *Let $1 \leq M \leq N$ be a divisor of N . Then $\boldsymbol{\psi} \in T^N$ is an (M, N) -pattern if and only if it is a global minimum of the potential*

$$U^{M,N}(\boldsymbol{\psi}) = \sum_{m=1}^M K_m U_m\tag{54}$$

with $K_m > 0$ for $m = 1, \dots, M - 1$ and $K_M < 0$, where

$$U_m(\boldsymbol{\psi}) = \frac{N}{2} |p_{m\boldsymbol{\psi}}|^2, \quad p_{m\boldsymbol{\psi}} \triangleq \frac{1}{mN} \sum_{j=1}^N e^{im\psi_j}.$$

Note the potential (54) requires all-to-all communication between the particles in order to compute the control law (52). An alternate potential (for which (M, N) -patterns are also critical points) is available for undirected and connected communication topologies.⁶ This potential is a quadratic form that depends on the Laplacian matrix of the communication graph. For example, we illustrate in Figure 5(a) a numerical simulation of the feedback stabilization of a time-splay formation using an undirected-ring communication topology. The splay pattern of time-phases $\boldsymbol{\psi}$ corresponds to a regular pattern of particle phases $\boldsymbol{\gamma}$ in which sequential particle phases are uniformly separated in time.

The following result provides an algorithm to stabilize a symmetric circular formation at a prescribed reference position. And, following the same procedure described at the end of Section IV, it also provides an algorithm to stabilize a symmetric circular formation centered

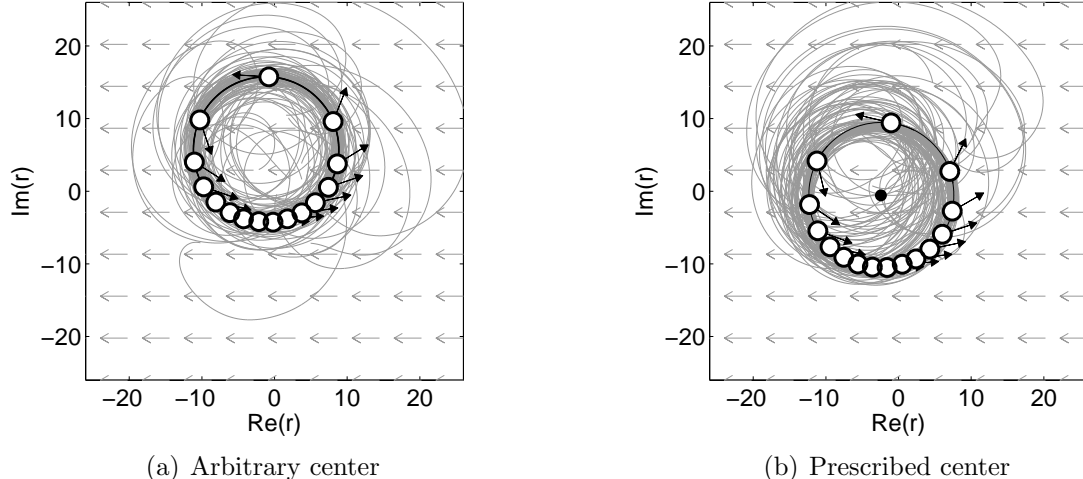


Figure 5. Stabilization of a time-splay circular formation using the control laws (52) and (55) with $N = 15$ and $\beta = -0.75$. The arrow attached to each particle represents its velocity relative to the flow. (a) Translation invariance in the closed-loop model (12) implies that the steady-state center of the formation is arbitrary. (b) Results of a numerical simulation in which the steady-state formation center is prescribed via a virtual particle to be $c_0 = -2.42 - 0.57i$.

on a moving target, provided the target is moving with constant velocity.

Corollary 2. Let $c_0 = r_0(0) + \omega_0^{-1}ie^{i\gamma_0(0)}$ be the fixed reference provided by a virtual particle, $k = 0$, whose dynamics are given by (39). Let $a_{k0} = 1$ equal one if particle k is informed of the reference and $a_{k0} = 0$ otherwise. If there is at least one informed particle, then all solutions of the particle model (12) with the control

$$\nu_k = \omega_0 s_k \left(1 + K \left(s_j \langle e^{i\gamma_k}, P_k \mathbf{e} \rangle + a_{k0} \langle e^{i\gamma_k}, c_k - c_0 \rangle - \frac{\partial U}{\partial \psi_k} \right) \right), \quad K > 0, \quad (55)$$

converge to a circular formation centered at c_0 with radius ω_0^{-1} and direction determined by the sign of ω_0 . Every isolated minimum of $U(\boldsymbol{\psi})$ defines an asymptotically stable set of circular formations. Every circular formation where $U(\boldsymbol{\psi})$ does not reach a minimum is unstable.

We illustrate Corollary 2 in Figure 5(b).

VI. Application Examples

To demonstrate the utility of the cooperative control algorithms presented above we describe two numerical simulations related to applications in environmental monitoring and target surveillance. In the first example, we illustrate how to coordinate multiple aerial vehicles such as the Aerosonde²⁴ in a simple model of a hurricane. An unmanned aircraft can observe a hurricane at a lower altitude than it is safe to fly a manned aircraft, and therefore

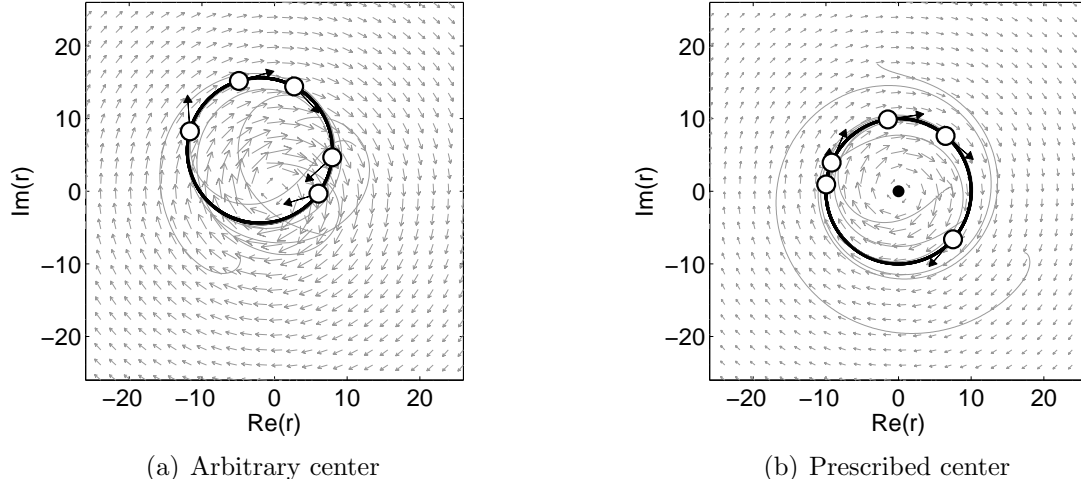


Figure 6. Stabilization of a circular formation in a simple hurricane model. The flow field is a modified Rankine vortex located at the origin with maximum wind speed equal to three times the particle speed relative to the flow. The arrow attached to each particle represents its velocity relative to the flow. (a) Translation invariance in the closed-loop model (12) implies that the steady-state center of the formation is arbitrary. (b) The steady-state formation center is prescribed to be at the center of the vortex, $c_0 = 0$.

presents an attractive option for improving hurricane forecasts via in-situ observations. In the second example, we illustrate how multiple aerial vehicles might converge to a time-splay formation centered on a constant-velocity target, even if the target maneuvers. This example provides an algorithm for coordinated tracking of a ground target in wind and without speed control. Such an algorithm is suitable for aerial surveillance/reconnaissance missions in which multiple sensing platforms must be coordinated. Each set of numerical results shows convergence of the closed-loop dynamics despite the fact that theoretical restrictions on flow speed and time-invariance are not enforced.

STABILIZATION OF A CIRCULAR FORMATION IN A SIMPLE HURRICANE MODEL In this example, we consider the problem of stabilizing a circular formation in the eyewall of a hurricane, where the wind speed vastly exceeds the platform speed. As a simple hurricane model, we use a modified *Rankine* vortex in which the tangential wind speed, v , varies with radius, r , according to two parameters—the maximum wind speed, v_m , and the radius, r_m , at which the maximum wind speed occurs. For $0 < r < r_m$, the wind profile is given by $v(r) = v_m(r/r_m)$; for $r \geq r_m$, $v(r) = v_m(r/r_m)^{-0.6}$. We simulate the particle model (12) with a Rankine vortex located at the origin with $v_m = 3$ (assuming unit particle speed relative to the flow) and $r_m = 1/(2\omega_0)$. Figure 6(a) illustrates the numerical results for the control (37), which stabilizes a circular formation at an arbitrary center position. Figure 6(b) illustrates the numerical results for the control (41), which stabilizes a circular formation centered on the vortex. This example illustrates an algorithm for coordination of hurricane observing platforms and suggests that the theoretical results may apply in flow fields whose magnitude

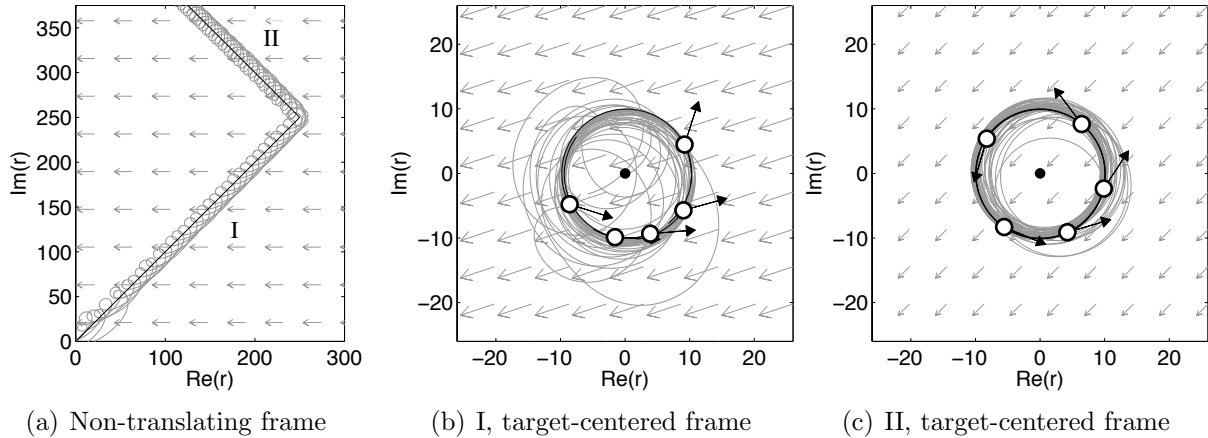


Figure 7. Stabilization of a time-splay formation centered on a moving target in a uniform flow. The target moves at constant velocity $b_0 = \pm 0.25 + 0.25i$ (assuming unit particle speed relative to the flow) and makes a single maneuver; the flow is uniform and has magnitude equal to half of the particle speed. The arrow attached to each particle represents its velocity relative to the flow. (a) Depiction of the tracking trajectories in an inertial frame that is not translating with the target. (b) Phase I of the tracking trajectories (before the maneuver) depicted in a target-centered reference frame. (c) Phase II of the tracking trajectories (after the maneuver) depicted in a target-centered reference frame.

exceeds the speed of the particle relative to the flow.

STABILIZATION OF A TIME-SPLAY FORMATION CENTERED ON A MOVING TARGET In this example, we consider the problem of stabilizing a time-splay formation of aerial vehicles centered on a moving target in the presence of a uniform flow field. We assume that the target moves with constant velocity between maneuvers. According to the discussion at the end of Section IV, we can use as an inertial frame a non-rotating reference frame fixed to the target. We establish such a frame for each constant-velocity portion of the target's trajectory. We simulate the particle model (45) with effective flow speed $f'_k = f_k - b_0$, where the flow field is $f_k = -0.5$ and the target velocity is $b_0 = \pm 0.25 + 0.25i$ (assuming unit vehicle speed relative to the flow). Note that the magnitude of the effective flow is less than the vehicle speed relative to the flow. The target makes a single, 90-degree turn. Figure 7(a) illustrates the numerical results in an inertial reference frame that is not translating with the target. Figure 7(b) uses a target-centered frame to illustrate the numerical results prior to the maneuver for the control (55), which stabilizes a time-splay formation centered on the target position. Figure 7(c) illustrates the numerical results in a target-centered frame after to the maneuver. The impact of the maneuver can be understood as a step function on the flow-field input. This example provides an algorithm for coordinated tracking of a moving target and suggests that the theoretical results may apply in a flow field that varies in time.

VII. Conclusions

Distributed sensing with multiple, mobile platforms is enhanced by cooperative-control algorithms that generate coordinated sampling trajectories in the presence of strong and variable flow fields. The design of these algorithms is based on simple models of platform motion that often ignore the presence of flow. In this paper, we describe a self-propelled particle model that explicitly incorporates the presence of a known, time-invariant flow field. We assume that the flow does not exceed the speed of a particle relative to the flow. We provide decentralized control algorithms that stabilize primitive collection motions including synchronized, balanced, circular, and symmetric circular formations. These motion primitives are essential to the construction of a systematic framework for autonomous and distributed sensing in the presence of flow, as has been illustrated in two numerical examples. In ongoing work, we focus on extending the framework described here to the nonautonomous dynamical systems that arise in the study of time-varying flows.

VIII. ACKNOWLEDGMENTS

We thank the anonymous reviewers for their insightful comments and suggestions. We also thank Sharan Majumdar for providing the simple hurricane model.

References

- ¹N. E. Leonard, D. A. Paley, F. Lekien, R. Sepulchre, D. M. Fratantoni, and R. E. Davis, "Collective motion, sensor networks and ocean sampling," *Proc. IEEE*, vol. 95, no. 1, pp. 48–74, 2007.
- ²E. W. Justh and P. S. Krishnaprasad, "A simple control law for UAV formation flying," Institute for Systems Research, University of Maryland, Tech. Rep. 2002-38, 2002. [Online]. Available: <http://techreports.isr.umd.edu/reports/2002/TR.2002-38.pdf>
- ³—, "Equilibria and steering laws for planar formations," *Systems and Control Letters*, vol. 52, no. 1, pp. 25–38, 2004.
- ⁴F. Zhang and N. E. Leonard, "Coordinated patterns of unit speed particles on a closed curve," *Systems and Control Letters*, vol. 56, no. 6, pp. 397–407, 2007.
- ⁵R. Sepulchre, D. A. Paley, and N. E. Leonard, "Stabilization of planar collective motion: All-to-all communication," *IEEE Trans. Automatic Control*, vol. 52, no. 5, pp. 811–824, 2007.
- ⁶—, "Stabilization of planar collective motion with limited communication," *IEEE Trans. Automatic Control*, vol. 53, no. 3, pp. 706–719, 2008.
- ⁷F. Zhang, D. M. Fratantoni, D. A. Paley, J. M. Lund, and N. E. Leonard, "Control of coordinated patterns for ocean sampling," *Int. J. Control*, vol. 80, no. 7, pp. 1186–1199, 2007.
- ⁸D. A. Paley, F. Zhang, and N. E. Leonard, "Cooperative control for ocean sampling: The Glider Coordinated Control System," *IEEE Trans. Control Systems Technology*, vol. 16, no. 4, pp. 735–744, 2008.
- ⁹D. A. Paley, "Cooperative control of collective motion for ocean sampling with autonomous vehicles,"

Ph.D. dissertation, Princeton University, Princeton, New Jersey, September 2007. [Online]. Available: <http://wam.umd.edu/~dpaley/papers/paley-thesis.pdf>

¹⁰——, “Stabilization of Collective Motion in a Uniform and Constant Flow Field,” in *Proc. AIAA Guidance, Navigation and Control Conf. and Exhibit*, no. AIAA-2008-7173, Honolulu, Hawaii, August 2008, (8 pages).

¹¹——, “Cooperative Control of an Autonomous Sampling Network in an External Flow Field,” to appear in *Proc. 47th IEEE Conf. Decision and Control*, Invited session on “Autonomous exploration and remote sensing”.

¹²L. Techy, D. A. Paley, and C. A. Woolsey, “UAV coordination on convex curves in wind: An environmental sampling application,” submitted.

¹³N. Ceccarelli, J. J. Enright, E. Frazzoli, S. J. Rasmussen, and C. J. Schumacher, “Micro UAV path planning for reconnaissance in wind,” in *Proc. 2007 American Control Conf.*, New York City, New York, July 2007, pp. 5310–5315.

¹⁴T. G. McGee, S. Spry, and J. K. Hedrick, “Optimal path planning in a constant wind with a bounded turning rate,” in *Proc. AIAA Conf. Guidance, Navigation, and Control (electronic)*, no. AIAA 2005-6186, San Francisco, California, August 2005, (11 pages).

¹⁵T. G. McGee and J. K. Hedrick, “Path planning and control for multiple point surveillance by an unmanned aircraft in wind,” in *Proc. 2006 Amer. Control Conf.*, Minneapolis, Minnesota, June 2006, pp. 4261–4266.

¹⁶R. Rysdyk, “Course and heading changes in significant wind,” *J. Guidance, Control, and Dynamics*, vol. 39, no. 4, pp. 1168–1171, 2007.

¹⁷L. Techy, C. A. Woolsey, and D. G. Schmale, “Path planning for efficient UAV coordination in aerobiological sampling missions,” to appear in *Proc. 47th IEEE Conf. Decision and Control*.

¹⁸D. J. Klein and K. A. Morgansen, “Controlled collective motion for trajectory tracking,” in *Proc. 2006 American Control Conf.*, Minneapolis, Minnesota, June 2006, pp. 5269–5275.

¹⁹R. Rysdyk, “Unmanned aerial vehicle path following for target observation in wind,” *J. Guidance, Control, and Dynamics*, vol. 29, no. 5, pp. 1092–1100, 2006.

²⁰D. B. Kingston, “Decentralized control of multiple UAVs for perimeter and target surveillance,” Ph.D. dissertation, Department of Electrical and Computer Engineering, Brigham Young University, Provo, Utah, December 2007. [Online]. Available: <http://www.ee.byu.edu/faculty/beard/papers/thesis/DerekKingstonPhD.pdf>

²¹E. W. Frew, D. A. Lawrence, and S. Morris, “Coordinated standoff tracking of moving targets using Lyapunov guidance vector fields,” *J. Guidance, Control, and Dynamics*, vol. 31, no. 2, pp. 290–306, 2008.

²²T. H. Summers and M. R. Akella, “Coordinated standoff tracking of moving targets: Control laws and information architectures,” in *Proc. AIAA Guidance, Navigation and Control Conf. and Exhibit (electronic)*, no. AIAA-2008-7021, Honolulu, Hawaii, 2008, (25 pages).

²³D. A. Paley, N. E. Leonard, and R. Sepulchre, “Stabilization of symmetric formations to motion around convex loops,” *Systems and Control Letters*, vol. 57, no. 3, pp. 209–215, 2008.

²⁴G. J. Holland, P. J. Webster, J. A. Curry, G. Tyrell, D. Gauntlett, G. Brett, J. Becker, R. Hoag, and W. Vaglianti, “The Aerosonde robotic aircraft: A new paradigm for environmental observations,” *Bull. American Meteorological Society*, vol. 82, no. 5, pp. 889–901, 2001.